Biological Sciences: Plant Biology

Ycf48 involved in the biogenesis of the oxygen-evolving photosystem II complex is a seven-bladed beta-propeller protein

Jianfeng Yu[1*], Jana Knoppová[2*], Franck Michoux[1], Wojciech Bialek[1†], Ernesto Cota[1], Mahendra K. Shukla[2], Adéla Strašková[2], Guillem Pascual Aznar[2], Roman Sobotka[2], Josef Komenda[2], James W. Murray[1] and Peter J. Nixon[1]

[1]Sir Ernst Chain Building-Wolfson Laboratories, Department of Life Sciences, Imperial College London, South Kensington Campus, London, SW7 2AZ UK

[2]Institute of Microbiology, Center Algatech, Opatovický mlýn, 37981 Třeboň, Czech Republic

[*]These authors contributed equally to this work

[†]Current address: Department of Biophysics, Faculty of Biotechnology, University of Wroclaw, Wroclaw, Poland

40926 characters

Corresponding author:

Jianfeng Yu, Sir Ernst Chain Building-Wolfson Laboratories, Department of Life Sciences, Imperial College London, S. Kensington Campus, London, SW7 2AZ, UK. E-mail: j.yu@imperial.ac.uk

Abstract (250 words)

Robust photosynthesis in chloroplasts and cyanobacteria requires the participation of accessory proteins to facilitate the assembly and maintenance of the photosynthetic apparatus located within the thylakoid membranes. The highly conserved Ycf48 protein acts early in the biogenesis of the oxygen-evolving photosystem II (PSII) complex by binding to newly synthesized precursor D1 subunit and by promoting efficient association with the D2 protein to form a PSII reaction center (PSII RC) assembly intermediate. Ycf48 is also required for efficient replacement of damaged D1 during the repair of PSII. However, the structural features underpinning Ycf48 function remain unclear. Here we show that Ycf48 proteins encoded by the thermophilic cyanobacterium *Thermosynechococcus elongatus* and the red alga *Cyanidioschyzon merolae* form seven-bladed beta-propellers with the 19 amino-acid insertion characteristic of eukaryotic Ycf48 located at the junction of blades 3 and 4. Knowledge of these structures has allowed us to identify a conserved 'Arg patch' on the surface of Ycf48 that is important for binding of Ycf48 to PSII RCs but also to larger complexes including trimeric photosystem I (PSI). Reduced accumulation of chlorophyll in the absence of Ycf48 and the association of Ycf48 with PSI provide evidence of a more wide-ranging role for Ycf48 in the biogenesis of the photosynthetic apparatus than previously thought. Co-purification of Ycf48 with the cyanobacterial YidC protein insertase supports the involvement of Ycf48 during the co-translational insertion of chlorophyll-binding apopolypeptides into the membrane.

Key words:

photosystem II, photosynthesis, chlorophyll-binding proteins

Significance statement (120 words)

The oxygen-evolving photosystem II (PSII) complex is essential for driving the light reactions of photosynthesis and for producing the oxygen we breathe. Accessory proteins, most of unknown function, are vital for assembling and maintaining PSII activity. Here we provide structural information on Ycf48/HCF136, which is involved in the early steps of PSII assembly and the repair of PSII following damage by light. We show that Ycf48 is a seven-bladed beta propeller and that a highly conserved arginine patch is important for function. We propose a role for Ycf48 in coordinating the binding of chlorophyll to protein during insertion of chlorophyll-binding proteins into the membrane. Our work provides new insights into the assembly of the photosynthetic apparatus used to harvest sunlight.

\body

Introduction

The photosystem II (PSII) complex found in the thylakoid membranes of cyanobacteria and chloroplasts is a multisubunit pigment-protein complex that uses light energy to drive the oxidation of water to oxygen and the reduction of plastoquinone to plastoquinol in oxygenic photosynthesis (1, 2). PSII is prone to light-induced damage *in vivo* and is repaired via the specific replacement of damaged protein subunits within the complex, especially the D1 reaction center subunit (3). Recent advances in determining the structures of PSII from both cyanobacteria (4) and chloroplasts (5, 6) make PSII an excellent model system to study both the assembly and repair of a thylakoid membrane protein complex at the molecular level.

PSII in cyanobacteria is assembled in the membrane in a stepwise fashion from smaller pigment-protein modules or sub-complexes composed of a major chlorophyll-binding subunit plus associated low-molecular-mass PSII subunits (3, 7). The PSII reaction center (PSII RC) assembly complex is formed from D1/PsbI and D2/Cyt b_{559} sub-complexes and is converted to the RC47 complex (8) by addition of the CP47 module (9); the monomeric PSII core complex is then formed by attachment of the CP43 module (3, 9). Formation of the holoenzyme involves light-driven assembly of the water-oxidizing Mn_4CaO_5 cluster, attachment of lumenal extrinsic proteins and dimerization, reviewed in (10).

Conserved accessory factors optimize assembly and/or repair of PSII following photodamage (3, 11, 12). Of these, Ycf48 (also known as HCF136 in plants) acts early in assembly and is important for formation of the PSII RC assembly complex in both plants (13, 14) and cyanobacteria (15). Ycf48 has been biochemically isolated as a component of cyanobacterial PSII RC assembly complexes (16) and stabilizes unassembled precursor D1 destined for either formation of the PSII RC during assembly or replacement of damaged D1 during PSII repair (15). Ycf48 is able to recognize the C-terminal extension of precursor D1 although this interaction is not crucial for assembly of the PSII RC (15). In the case of chloroplasts, many Ycf48/HCF136 contain a characteristic insertion of 19 amino-acid residues of unknown function (13). Despite its physiological importance, the structural features of Ycf48 that are important for function remain unknown.

We show here that Ycf48 encoded by the thermophilic cyanobacterium *Thermosynechococcus elongatus* and the thermophilic red alga *Cyanidioschyzon merolae* is a seven-bladed beta propeller and identify a highly conserved positively charged region (so-called ‘Arg patch’) that is important for attachment of Ycf48 to PSII. Surprisingly, we find that

Ycf48 also binds to photosystem I (PSI) consistent with a direct role for Ycf48 in the accumulation of PSI not just PSII. Based on the co-purification of Ycf48 with the YidC insertase involved in the insertion of proteins into the thylakoid membrane, and the requirement for Ycf48 for normal chlorophyll biosynthesis, we propose that Ycf48 binds to chlorophyll-binding apopolypeptides as they are released into the membrane, possibly to help coordinate protein insertion and folding with loading of chlorophyll molecules into their binding sites.

Results

Ycf48 binds to large PSI and PSII complexes

In previous work we used 2D electrophoresis combined with immunoblotting to demonstrate that the Ycf48 protein in the cyanobacterium *Synechocystis* sp. PCC 6803 (hereafter *Synechocystis*) is a component of two types of PSII RC assembly complex, designated PSII RCII* and PSII RCa (15–17). PSII RCII* is larger than the PSII RCa complex as it also contains the Ycf39/Hlip complex involved in chlorophyll delivery (16). The antibody we originally used to detect Ycf48 was raised against Ycf48 from *Arabidopsis* (15). To determine whether Ycf48 was also present at low abundance in other complexes, we repeated the analysis using a more sensitive antibody raised against *Synechocystis* Ycf48 and by using clear native-polyacrylamide gel electrophoresis (CN-PAGE) rather than blue native (BN)-PAGE in the first dimension. Ycf48 was now detected in several larger complexes (Fig. 1). Based on the analysis of mutants unable to assemble PSI (a ΔPSI mutant lacking both the PsaA and PsaB RC subunits) or blocked at various stages of PSII assembly (in strains lacking either CP43 or CP47) (Fig. S1), we tentatively assigned these larger complexes as monomeric and dimeric core complexes of PSII (18) and monomeric and trimeric complexes of PSI (Fig. 1).

The apparent binding of Ycf48 to PSI was intriguing as Ycf48 has so far been considered a PSII-specific accessory factor. To provide additional evidence for an interaction with PSI *in vivo*, PSI complexes were isolated from a *Synechocystis* strain expressing YFP-tagged PsaF by immunoaffinity chromatography (19). Ycf48 was detected in the YFP-tagged PSI complexes by immunoblotting, especially the trimer, but was barely detectable in the wild-type (WT) control (Fig. 2). Likewise, pull-down experiments, using various types of His-tagged PSII complex (8, 9), confirmed the association of Ycf48 with His-tagged CP47 and with larger PSII complexes containing His-tagged CP47 (Fig. S2A,B).

We also obtained experimental support for the lumenal location of cyanobacterial Ycf48 following trypsin digestion of intact right-side out thylakoids (Fig. S2C), in agreement with an earlier characterization of the spinach Ycf48 homologue (13). In summary, these results showed that Ycf48 was able to bind to the lumenal side of larger PSI and PSII complexes not just PSII RC assembly complexes.

Structure of Ycf48 from *T. elongatus* and *C. merolae*

To gain insights into the mechanism of Ycf48 function, we solved the crystal structure of recombinant Ycf48 from the thermophilic cyanobacterium *Thermosynechococcus elongatus,* which is widely used for structural studies (20, 21), to a resolution of 1.5 Å (Fig. 3A). Ycf48 is a seven-bladed beta propeller, in an approximate torus shape with width ~50 Å and depth ~25 Å. Seven 'blades' of four-stranded beta sheets are arranged around the axis, with a central pore. Ycf48 has the beta-propeller 'Velcro', where the final beta-strand of the C-terminal blade comes from the N-terminal end of the protein. The beta-propeller fold is common, with examples known with four to ten blades. Some beta-propellers are enzymes, but many have scaffolding roles in larger protein complexes (22). The most similar structure in the PDB to *T. elongatus* Ycf48 is an antibiotic degrading enzyme, virginiamycin B lyase, Vgb (23), with a root-mean-square deviation (RMSD) of 3.7 Å over 272 residues but the active site residues of Vgb are not present in Ycf48. We do not predict any enzyme activity for Ycf48.

Eukaryotic Ycf48 sequences have a 19 amino-acid insertion compared with cyanobacterial Ycf48 (13). We also determined the crystal structure of Ycf48 from the thermophilic red alga *Cyanidioschyzon merolae*. *C. merolae* Ycf48 showed the same seven–bladed structure as *T. elongatus* Ycf48 with the 19 amino-acid insert, consisting of two short alpha helices and two turns, located between blades three and four (Fig. 3B). The three other small insertions seen in *C. merolae* Ycf48 (E161-E164, N322-A324 and N345-S348) compared with *T. elongatus* Ycf48 are also found in loop regions exposed to the surface (Fig. S3). Some Ycf48 sequences have inserts in other regions of the protein (Fig. S3B). Based on the structures reported here, most of these inserts are again predicted to lie in between conserved blade sheet regions (Fig. S3B).

To test the physiological effect of the 19-residue insert in *Synechocystis*, which is widely used for mutagenesis studies, we created a mutant, Ycf48-CM, in which the 19 residue insert from *C. merolae* was inserted into the endogenous Ycf48 protein of *Synechocystis*. No effect was observed as the Ycf48-CM mutant grew as well as WT at high irradiances (Fig. S4A), had WT levels of chlorophyll (Fig. S4B) and could still bind to the

photosynthetic complexes as assessed by 2D gel electrophoresis and immunoblotting (Fig. S4C).

A conserved Arg patch is important for binding of Ycf48

The conservation of the Ycf48 structures was analyzed using ConSurf (24, 25), which maps residue conservation scores to the structure. The most conserved region on the surface of *T. elongatus* Ycf48 was a patch of four Arg residues (202, 221, 225 and 226, *T. elongatus* numbering) on blade four and five on what we designate as the top surface of the beta-propeller (Fig. 4A). To investigate the importance of this region, we made a quadruple mutant of *Synechocystis* in which all four Arg-patch residues were mutated to Glu (mutant Ycf48-REquad). The homologous Arg residues in *Synechocystis* are R196, R215, R219 and R220. The Ycf48-REquad mutant was chlorophyll deficient like the *ycf48* deletion strain (Fig. S4B) and was unable to grow photoautotrophically at high irradiance suggesting loss of function (Fig. 5A, Fig. S4A). 2D gel electrophoresis revealed that Ycf48 accumulated in the Ycf48-REquad mutant, but showed impaired binding to the photosynthetic complexes (Fig. 5B). Pulse-labeling cells with [^{35}S]-Met/Cys and subsequent analysis of newly synthesized membrane proteins confirmed that the assembly of PSII complexes was impaired at an early stage of biogenesis in the Ycf48-REquad mutant (Fig. 5B) similar to the *ycf48* null mutant (15). Radiolabeled D1 was detected mainly in an unassembled state whereas in WT more D1 was incorporated into larger PSII complexes. Mutating the four Arg residues to Ala (in mutant Ycf48-RAquad) also increased susceptibility of growth to light stress and reduced levels of chlorophyll per cell, but to a lesser extent than the Ycf48-REquad mutant (Fig. S4A,B), despite WT levels of Ycf48 (Fig. S7D).

To assess possible indirect effects of the mutations on the folding of Ycf48, the structure of recombinant *T. elongatus* Ycf48-REquad was determined by X-ray crystallography. The structure was similar to the WT (RMSD 0.75 Å), except for local changes around the cluster of four arginines, implying no dramatic changes in the tertiary structure of Ycf48 in the quadruple mutant *in vivo* (Fig. 4B).

In contrast to the Ycf48-REquad mutant, the single arginine to glutamate mutants behaved like the WT control strain and could grow at high irradiance suggesting that binding of Ycf48 was dependent on two or more Arg residues in the patch (Fig. 5A). The functional importance of each Arg residue was further assessed by mutating each of the four Glu residues in the Ycf48-REquad mutant back to Arg to generate four triple mutants. Growth tests at increasing irradiances revealed that restoring R196 or R220 alone conferred better resistance to light stress than that of R215 and R219, although none of the triple mutants

was able to grow when the irradiance reached 90-130 µE m^{-2} s^{-1}, indicating reduced fitness compared to the WT control strain (Fig. 5A). In all triple mutants Ycf48 was expressed at WT levels (Fig. S7D).

Analysis of the *T. elongatus* Ycf48 structure revealed that the equivalent residues to R196 and R220 in *Synechocystis* sit on the top-surface of Ycf48, with side-chains pointing upward, while the equivalent residues to R215 and R219 lie slightly to the side (Fig. 4A, Fig. S5). R220 was observed in two conformations in the electron density, showing flexibility. Overall our data identify an important role for the Arg patch in binding to both PSI and PSII complexes, and provide evidence for differences in the functional importance of the four Arg residues.

Ycf48 co-purifies with YidC and the phenotype of the null mutant can be suppressed by increased chlorophyll availability

A role for Ycf48 at an early stage of biogenesis of PSII raised the possibility that the blades of Ycf48 might engage with lumenally exposed regions of newly synthesized proteins as they are co-translationally inserted into membrane. The D1 subunit of PSII enters into the membrane via the ALB3 insertase in chloroplasts (26) and its homologue, YidC, in cyanobacteria (27). To test for the association of Ycf48 and, possibly, other assembly factors with YidC in *Synechocystis*, pull-down experiments using an anti-FLAG antibody were performed with detergent-solubilized extracts isolated from a C-terminal Flag-tagged derivative of YidC (YidC-FLAG) (28). YidC-FLAG was immunopurified and, importantly, both Ycf48 and CyanoP, the latter shown recently to bind to D2 at an early stage of assembly of PSII (29), were co-eluted with YidC-FLAG (Fig. 6). FtsH protease subunits (FtsH2 and FtsH3) and the Band 7 protein, Phb1, also co-purified with YidC-FLAG, which is consistent with earlier experiments showing co-purification of FtsH and the Band 7 proteins HflK/C with *Escherichia coli* YidC in cross-linking experiments (30). In contrast, CyanoQ (21), PAM68/Sll0933 (31), Psb27 (32), Psb28 (33) and Psb28-2 (34), which are all involved in PSII assembly/repair, were not detected in the YidC-FLAG eluate by either immunoblotting or mass spectrometry.

It has been shown recently that the Ycf48 protein is particularly important when chlorophyll availability in the cell is low: a point mutation in the Mg-chelatase enzyme, which produces Mg-protoporphyrin IX for chlorophyll biosynthesis, abolished photoautotrophic growth of a Ycf48 deletion mutant, whereas there was no significant effect on growth in the WT background (35). As these results indicated a tight link between the function of Ycf48 and chlorophyll biosynthesis, we analyzed intermediates of the chlorophyll synthesis

pathway in the *ycf48* null mutant using HPLC. Our analysis showed that chlorophyll precursors were substantially reduced compared to WT (Fig. 7A).

To assess the effect of a better chlorophyll supply on the phenotype of the *ycf48* null mutant, liquid and solid cultures were supplemented with N-methyl mesoporphyrin IX, a potent and specific inhibitor of the ferrochelatase enzyme, whose partial inhibition has been shown to increase chlorophyll biosynthesis (36). After one-day treatment with inhibitor the *ycf48* null mutant accumulated high levels of chlorophyll precursors (Fig. 7B), showed improved growth (Fig. 7C) and enhanced levels of chlorophyll per cell (Fig. 7D). Analysis by CN-PAGE indicated increased levels of both trimeric PSI and dimeric PSII complexes (Fig. 7E).

Discussion

A number of accessory factors involved in the assembly and maintenance of the thylakoid membrane have now been identified, mainly through genetic studies (reviewed in (12)). However, there is little information on the structural features of these proteins that are important for function. We show here that Ycf48 from both cyanobacteria and chloroplasts forms a seven-bladed beta propeller. The beta propeller structural motif is found widely in nature both in enzymes and in structural proteins involved in the assembly of larger protein complexes, with individual blades helping to mediate protein-protein interactions (reviewed in (37)). This latter function is consistent with the known role for Ycf48 in orchestrating the assembly of PSII in cyanobacteria. Besides binding to unassembled D1 (15), Ycf48 is thought to interact with CyanoP, pre-bound to D2, to promote assembly of the PSII RC assembly complex (29) and with PAM68/Sll0933 to form larger PSII complexes (31, 38).

Using the Ycf48 crystal structures, we identified a conserved patch of arginine residues as a region to investigate further. A role in binding to the lumenal surfaces of thylakoid membrane complexes was revealed through analysis of a quadruple mutant in which all four Arg residues were replaced by Glu. The lack of a significant growth defect at high irradiances in the single Arg mutants suggests that the functionality of Arg patch is a collective property of two or more residues. Further analysis on triple Arg to Glu mutants in *Synechocystis* revealed that R196 and R220 are functionally more important than R215 and R219, which suggests that the top surface of the Arg patch has greater importance for binding (Fig. 4A, Fig. S5).

An interaction between Ycf48 and the 16 amino-acid long C-terminal extension of precursor of D1, which is proteolytically cleaved after formation of the PSII RC to form an intermediate form of D1 (iD1) with an 8 amino-acid extension (39), has previously been

suggested from yeast-2-hybrid experiments (15). We have been able to co-crystallize *T. elongatus* Ycf48 with two peptides corresponding to D1. Firstly the mD1 peptide (NAHNFPLDLA), corresponding to residues 335-344 of the mature D1 protein (Fig. S6A) and secondly the iD1 peptide (NAHNFPLDLASAESAPVA) corresponding to residues 335-352 of the precursor D1 protein (39)(Fig. S6B,C). Three potential binding sites were identified with the binding site for the extended iD1 peptide starting close to the Arg patch (Fig. S6). However, the physiological relevance of these sites is unknown as we have so far been unable to find conditions to detect peptide binding to isolated Ycf48 by NMR or isothermal calorimetry to allow the candidate peptide-binding sites to be probed by mutagenesis.

Binding of chlorophyll synthase, the final enzyme involved in chlorophyll biosynthesis, to YidC is essential for co-translational insertion of chlorophyll into the nascent polypeptide chains of newly synthesized chlorophyll-binding proteins (28). The co-purification of Ycf48 with a FLAG-tagged version of *Synechocystis* YidC (Fig. 6) and partial suppression of the absence of Ycf48 by increased chlorophyll supply (Fig. 7) therefore suggest that Ycf48 is pre-bound to YidC and might assist YidC during the synthesis of chlorophyll-binding proteins. Extending previous ideas on the role of Ycf48/HCF136 in chloroplasts (14), we suggest that the blades of Ycf48 might interact with emerging lumenal parts of the newly synthesized membrane proteins, possibly via coulombic interactions with the Arg patch, to allow efficient and precise incorporation of pigments and other cofactors into the transmembrane regions (Fig. 8). The 19-residue insert exclusive to eukaryotes does not impair function of Ycf48 in cyanobacteria (Fig. S4) and so might play a specific role in eukaryotes, such as interacting with Alb3, which has clear sequence differences to YidC in prokaryotes (40).

Our detection of Ycf48 in larger PSII core complexes might reflect retention of Ycf48 on the lumenal surface of PSII prior to light-driven assembly of the oxygen-evolving complex. Control immunoblots showed that neither YidC nor PAM68/Sll0933 was present in large PSII complexes resolved by native gel electrophoresis suggesting that Ycf48 is not attached to PSII via either of these components. Given that Ycf48 associates with unassembled D1, a plausible site of interaction is between the Arg patch of Ycf48 and the negatively charged residues on the lumenal surface of D1 including those that ultimately ligate the oxygen-evolving Mn_4CaO_5 cluster. In this scenario Ycf48 maintains D1 in a competent state for assembly of the Mn cluster and attachment of the lumenal proteins. Alternatively, binding of Ycf48 to larger PSII complexes might reflect an early stage of repair in which Ycf48 associates with damaged PSII.

It is not clear why the Ycf48 knock-out mutant exhibits strongly down-regulated chlorophyll biosynthesis, as this seems to be essentially the opposite response that is required if the cell is to accumulate more chlorophyll-protein complexes in the absence of Ycf48. Restricted chlorophyll biosynthesis has, however, been reported for other PSII mutants (36) and so it appears that there is a feedback mechanism that co-ordinates *de novo* chlorophyll synthesis with PSII assembly/repair. In this way the levels of free chlorophyll and chlorophyll precursors, which can lead to the light-induced production of reactive oxygen species, can be controlled. Although detection of Ycf48 in PSI complexes implies a direct role for Ycf48 in PSI assembly, the reduced level of PSI (Fig. 7E) in the Ycf48 mutant might also be partly caused by a limitation in chlorophyll supply. Previous work has shown that PSI complexes are the main sink for newly synthesized chlorophyll in *Synechocystis* (41) and that PSI accumulation is sensitive to the availability of chlorophyll (42).

Materials and Methods

Details of the construction of *Synechocystis* strains, cultivation conditions, photometric measurements of cells and chlorophyll, HPLC analysis of chlorophyll-derived pigments and precursors, preparation of cellular membranes, isolation of YidC-FLAG and PSI-YFP through affinity chromatography, protein electrophoresis, immunoblotting and radiolabelling are described in SI Materials and Methods. Work related to the structural studies of Ycf48, including construction of expression vectors, protein expression, purification, X-ray crystallography and data processing is also described in SI Materials and Methods.

Acknowledgements

We would like to thank Martin Walsh for assistance at ESRF-BM14. We thank Diamond Light Source for access to beamlines I03 and I04 (mx7299 and mx12579) that contributed to the results presented here. J.W.M. was funded for part of this work by a BBSRC David Phillips Fellowship (BB/F023308/1). J.Y., F.M., W.B., P.J.N., J.W.M. and E.C. are grateful to the BBSRC for funding this work (BB/I00937X/1 and BB/L003260/1). J.Knop., M.K.S, A.S., G.P.A., R.S. and J.K. were supported by the projects 17-08755S and P501/12/G055 of the Czech Science Foundation and by the Czech Ministry of Education (projects CZ 1.05/2.1.00/19.0392, LO1416 and LM2015055).

References

1. Diner BA, Rappaport F (2002) Structure, dynamics, and energetics of the primary photochemistry of photosystem II of oxygenic photosynthesis. *Annu Rev Plant Biol* 53:551–580.

2. Barber J (2016) Photosysten II: the water splitting enzyme of photosynthesis and the origin of oxygen in our atmosphere. *Q Rev Biophys* 49:e14.

3. Komenda J, Sobotka R, Nixon PJ (2012) Assembling and maintaining the photosystem II complex in chloroplasts and cyanobacteria. *Curr Opin Plant Biol* 15(3):245–251.

4. Shen J-R (2015) The structure of photosystem II and the mechanism of water oxidation in photosynthesis. *Annu Rev Plant Biol* 66:23–48.

5. Wei X, et al. (2016) Structure of spinach photosystem II–LHCII supercomplex at 3.2 Å resolution. *Nature* 534(7605):69–74.

6. van Bezouwen LS, et al. (2017) Subunit and chlorophyll organization of the plant photosystem II supercomplex. *Nat plants* 3(7):17080.

7. Heinz S, Liauw P, Nickelsen J, Nowaczyk M (2016) Analysis of photosystem II biogenesis in cyanobacteria. *Biochim Biophys Acta - Bioenerg* 1857(3):274–287.

8. Boehm M, et al. (2012) Subunit composition of CP43-less photosystem II complexes of *Synechocystis* sp. PCC 6803: implications for the assembly and repair of

photosystem II. *Philos Trans R Soc B Biol Sci* 367(1608):3444–3454.

9. Boehm M, et al. (2011) Investigating the early stages of photosystem II assembly in *Synechocystis* sp. PCC 6803: isolation of CP47 and CP43 complexes. *J Biol Chem* 286(17):14812–14819.

10. Bao H, Burnap RL (2016) Photoactivation: the light-driven assembly of the water oxidation complex of photosystem II. *Front Plant Sci* 7:1–13.

11. Nixon PJ, Michoux F, Yu J, Boehm M, Komenda J (2010) Recent advances in understanding the assembly and repair of photosystem II. *Ann Bot* 106(1):1–16.

12. Nickelsen J, Rengstl B (2013) Photosystem II assembly: from cyanobacteria to plants. *Annu Rev Plant Biol* 64:609–35.

13. Meurer J, Plücken H, Kowallik K V, Westhoff P (1998) A nuclear-encoded protein of prokaryotic origin is essential for the stability of photosystem II in *Arabidopsis thaliana*. *EMBO J* 17(18):5286–5297.

14. Plücken H, Müller B, Grohmann D, Westhoff P, Eichacker LA (2002) The HCF136 protein is essential for assembly of the photosystem II reaction center in *Arabidopsis thaliana*. *FEBS Lett* 532(1–2):85–90.

15. Komenda J, et al. (2008) The cyanobacterial homologue of HCF136/YCF48 is a component of an early photosystem II assembly complex and is important for both the efficient assembly and repair of photosystem II in *Synechocystis* sp. PCC 6803. *J Biol Chem* 283(33):22390–22399.

16. Knoppová J, et al. (2014) Discovery of a chlorophyll binding protein complex involved in the early steps of photosystem II assembly in *Synechocystis*. *Plant Cell* 26(3):1200–1212.

17. Dobáková M, Tichy M, Komenda J (2007) Role of the PsbI protein in photosystem II assembly and repair in the cyanobacterium *Synechocystis* sp. PCC 6803. *Plant Physiol* 145(4):1681–91.

18. Komenda J, et al. (2004) Accumulation of the D2 protein is a key regulatory step for assembly of the photosystem II reaction center complex in *Synechocystis* PCC 6803. *J Biol Chem* 279(47):48620–48629.

19. Strašková A, Knoppová J, Komenda J (2018) Isolation of the cyanobacterial YFP-tagged photosystem I using *GFP-Trap®*. *Photosynthetica* 56:300–305.

20. Michoux F, Takasaka K, Boehm M, Nixon PJ, Murray JW (2010) Structure of CyanoP at 2.8 Å: implications for the evolution and function of the PsbP subunit of photosystem II. *Biochemistry* 49(35):7411–7413.

21. Michoux F, et al. (2014) Crystal structure of CyanoQ from the thermophilic cyanobacterium *Thermosynechococcus elongatus* and detection in isolated photosystem II complexes. *Photosynth Res* 122(1):57–67.

22. Chaudhuri I, Söding J, Lupas AN (2008) Evolution of the β-propeller fold. *Proteins Struct Funct Genet* 71(2):795–803.

23. Korczynska M, Mukhtar TA, Wright GD, Berghuis AM (2007) Structural basis for streptogramin B resistance in *Staphylococcus aureus* by virginiamycin B lyase. *Proc Natl Acad Sci U S A* 104(25):10388–93.

24. Glaser F, et al. (2003) ConSurf: identification of functional regions in proteins by surface-mapping of phylogenetic information. *Bioinformatics* 19(1):163–164.

25. Ashkenazy H, et al. (2016) ConSurf 2016: an improved methodology to estimate and visualize evolutionary conservation in macromolecules. *Nucleic Acids Res* 44(W1):W344–W350.

26. Ossenbühl F, et al. (2004) Efficient assembly of photosystem II in *Chlamydomonas reinhardtii* requires Alb3.1p, a homolog of *Arabidopsis* ALBINO3. *Plant Cell* 16(7):1790–1800.

27. Ossenbühl F, Inaba-Sulpice M, Meurer J, Soll J, Eichacker LA (2006) The *Synechocystis* sp PCC 6803 Oxa1 homolog is essential for membrane integration of reaction center precursor protein pD1. *Plant Cell* 18(9):2236–2246.

28. Chidgey JW, et al. (2014) A cyanobacterial chlorophyll synthase-HliD complex associates with the Ycf39 protein and the YidC/Alb3 insertase. *Plant Cell* 26(3):1267–79.

29. Knoppová J, Yu J, Konik P, Nixon PJ, Komenda J (2016) CyanoP is involved in the early steps of Photosystem II assembly in the cyanobacterium *Synechocystis* sp. PCC 6803. *Plant Cell Physiol* 57(9):1921–1931.

30. van Bloois E, et al. (2008) Detection of cross-links between FtsH, YidC, HflK/C suggests a linked role for these proteins in quality control upon insertion of bacterial inner membrane proteins. *FEBS Lett* 582(10):1419–1424.

31. Armbruster U, et al. (2010) The *Arabidopsis* thylakoid protein PAM68 is required for efficient D1 biogenesis and photosystem II assembly. *Plant Cell* 22(10):3439–3460.

32. Nowaczyk MM, et al. (2006) Psb27, a cyanobacterial lipoprotein, is involved in the repair cycle of photosystem II. *Plant Cell* 18(11):3121–3131.

33. Dobáková M, Sobotka R, Tichý M, Komenda J (2008) Psb28 protein is involved in the biogenesis of the photosystem II inner antenna CP47 (PsbB) in the cyanobacterium *Synechocystis* sp. PCC 6803. *Plant Physiol* 149(2):1076–1086.

34. Bečková M, et al. (2017) Association of Psb28 and Psb27 proteins with PSII-PSI supercomplexes upon exposure of *Synechocystis* sp. PCC 6803 to high light. *Mol Plant* 10(1):62–72.

35. Crawford TS, Eaton-Rye JJ, Summerfield TC (2016) Mutation of Gly195 of the ChlH Subunit of Mg-chelatase Reduces Chlorophyll and Further Disrupts PS II Assembly in a Ycf48-Deficient Strain of Synechocystis sp. PCC 6803. *Front Plant Sci* 7:1060.

36. Sobotka R, Komenda J, Bumba L, Tichý M (2005) Photosystem II assembly in CP47 mutant of *Synechocystis* sp. PCC 6803 is dependent on the level of chlorophyll precursors regulated by ferrochelatase. *J Biol Chem* 280(36):31595–31602.

37. Chen CKM, Chan NL, Wang AHJ (2011) The many blades of the β-propeller proteins: conserved but versatile. *Trends Biochem Sci* 36(10):553–561.

38. Rengstl B, Knoppová J, Komenda J, Nickelsen J (2013) Characterization of a *Synechocystis* double mutant lacking the photosystem II assembly factors YCF48 and Sll0933. *Planta* 237(2):471–480.

39. Komenda J, et al. (2007) Cleavage after residue Ala352 in the C-terminal extension is an early step in the maturation of the D1 subunit of photosystem II in *Synechocystis*

PCC 6803. *Biochim Biophys Acta - Bioenerg* 1767(6):829–837.

40. Yen MR, Harley KT, Tseng YH, Saier MH (2001) Phylogenetic and structural analyses of the Oxa1 family of protein translocases. *FEMS Microbiol Lett* 204(2):223–231.

41. Kopečná J, Komenda J, Bučinská L, Sobotka R (2012) Long-term acclimation of the cyanobacterium *Synechocystis* sp. PCC 6803 to high light is accompanied by an enhanced production of chlorophyll that is preferentially channeled to trimeric photosystem I. *Plant Physiol* 160(4):2239–2250.

42. Kopečná J, Sobotka R, Komenda J (2013) Inhibition of chlorophyll biosynthesis at the protochlorophyllide reduction step results in the parallel depletion of photosystem I and photosystem II in the cyanobacterium *Synechocystis* PCC 6803. *Planta* 237(2):497–508.

43. Pilný J, Kopečná J, Noda J, Sobotka R (2015) Detection and quantification of heme and chlorophyll precursors using a high performance liquid chromatography (HPLC) system equipped with two fluorescence detectors. *Bio-Protocol* 5(3):e1390.

Figure legends

Fig. 1 Analysis of YCF48-containing complexes in membranes of WT *Synechocystis*. Membranes isolated from WT cells cultivated at 40 µE m^{-2} s^{-1} were analyzed by 2D-Clear Native/SDS-PAGE electrophoresis and the gel was stained by SYPRO Orange, photographed, blotted to a PVDF membrane and probed with a specific antibody raised to Ycf48 from *Synechocystis* (segment of the 2D blot with the specific antibody signal is shown). Pigmented complexes were detected in the first dimension by their color (1D color) and fluorescence (1D fluor). Designation of complexes in the SYPRO-stained gel: PSI(1), monomeric PSI complex; PSI(3), trimeric PSI complex; RCC(2) and RCC(1), dimeric and monomeric PSII core complexes, respectively; RC47, PSII core complex lacking CP43; U.P., unassembled proteins. In the case of the immunoblot, the migration of PSI and PSII complexes containing Ycf48 are designated by an asterisk. RCII* and RCIIa are reaction center assembly complexes previously shown to contain Ycf48 (15, 16). Thylakoid membranes containing 4 µg chlorophyll were analyzed.

Fig. 2 Identification of the Ycf48 protein in YFP-tagged PSI complexes isolated by a single step GFP-Trap affinity pull-down. (A) GFP-Trap preparations pulled down from the strain expressing PsaF-YFP (PSI-YFP) and from the WT strain were eluted by hot SDS and analyzed by 1D SDS-PAGE. The gels were stained by SYPRO Orange, blotted to a PVDF membrane and Ycf48, PsaD and D1 were consecutively detected using specific antibodies (segment of the blot with the specific antibody signal is shown). 2 µg of chlorophyll were loaded for WT and *ycf48*$^{-}$ membranes, 15 µl of SDS-eluted pull-downs (50% of the sample) were loaded for each GFP-Trap sample. (B) 2D-Clear Native/SDS-PAGE analysis of the GFP-Trap pulldowns from the PSI-YFP and WT strains eluted by low pH (glycine buffer pH=2.5) and immediately neutralized by Tris buffer. 15 µl of low pH-eluted pull-downs (50% of the sample) were analyzed by Clear Native-PAGE, lanes cut and re-electrophoresed in the second dimension. The 2D gels were stained by SYPRO Orange, blotted to a PVDF membrane and Ycf48 and D1 were consecutively detected using specific antibodies (segment of the blot containing individual antibody signals is shown).

Fig. 3 Structure of Ycf48 from cyanobacteria and red algae. Ribbon diagram representation of the structure of Ycf48 from *T. elongatus* (PDB ID: 2XBG)(A) and *C. merolae* (PDB ID: 5OJ3)(B), color gradient blue at the N-terminus to orange at the C-terminus. The 19-residue insert exclusive to eukaryotic Ycf48 is shown in purple. The blades are numbered along the direction of translation, with the ‘top’ of the protein defined as the view that gives an anticlockwise arrangement of the blades.

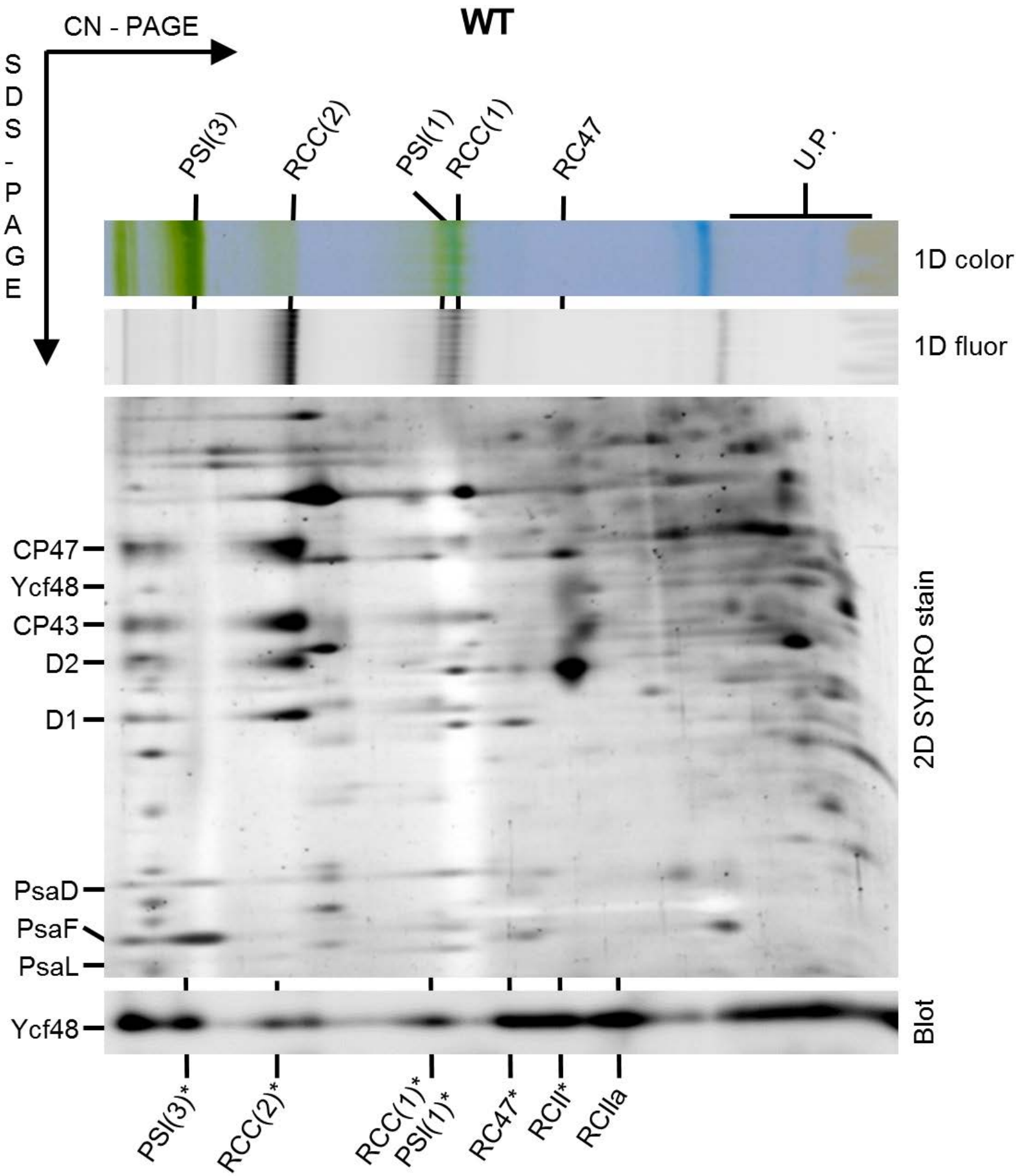
Fig. 4 Structural conservation and charge distribution of Ycf48 across cyanobacteria. (A) Different views of Ycf48 (PDB ID: 2XBG) displaying degree of residue conservation as deduced by a ConSurf (20) analysis of 122 cyanobacteria species; the sequence conservation score ranges from purple (high) to cyan (low). The position of the four conserved Arg residues are indicated with black lines. Two conformations of the side chain of R220 are modelled into the crystal structure. (B) Structural comparison of Ycf48-REquad (PDB ID: 5OJP) with native Ycf48. The charge distribution on the surface of WT containing the 4 arginine residues (left) and Ycf48-REquad (middle) containing the 4 glutamate substitutions are displayed; note the switch from positive (blue) to negatively charged (red) surface in the 'Arg patch' region (circled). The right panel shows the alignment of the alpha carbons in Ycf48-REquad and native Ycf48 and the side-chain positions of the four Arg (blue) and four Glu substitutions (red).

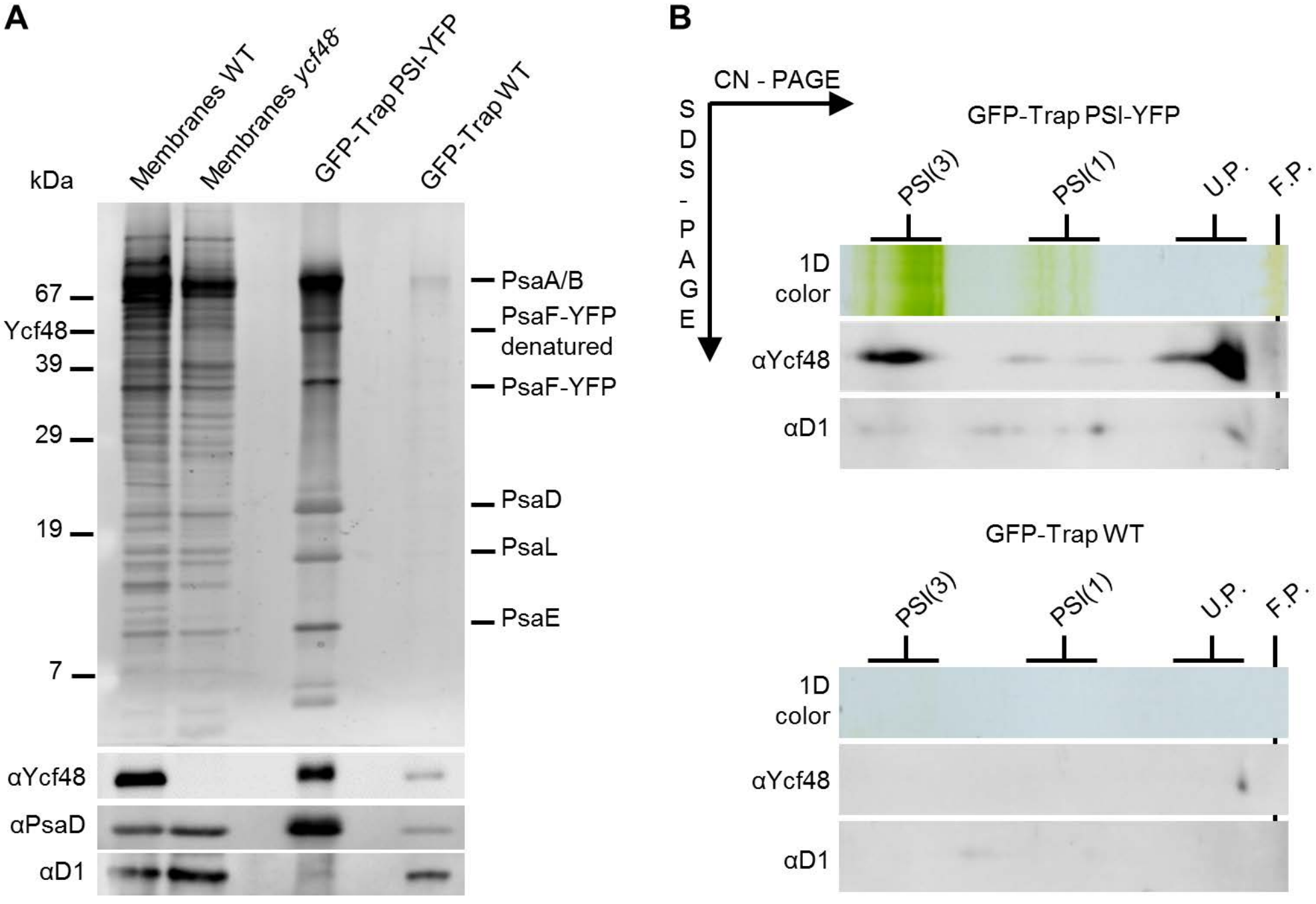
Fig. 5 Analysis of Ycf48-RE mutants. (A) Cell cultures were spotted on BG-11 plates and grown at low irradiance (40-50 µE m^{-2} s^{-1}, top row), semi-high irradiance (70-90 µE m^{-2} s^{-1}, middle row) and high irradiance (90-130 µE m^{-2} s^{-1}, bottom row). Strains analysed included WT, WT control carrying the downstream gentamycin-resistance marker, but expressing native Ycf48 (Ycf48-WT), Ycf48 knockout strain (ΔYcf48), Ycf48 with single Arg replaced with Glu (Ycf48-RxxxE), Ycf48 with all four Arg replaced with Glu (Ycf48-REquad) and Ycf48 with three of the four Arg replaced with Glu (Ycf48-ExxxRtrip, the number representing the Arg not mutated to Glu). Results of two separate growth experiments are shown. (B) Membranes (4 µg chlorophyll each) isolated from WT, Ycf48-REquad and Ycf48 knockout mutant (*ycf48*$^-$) subjected to radioactive pulse-labelling were analyzed by 2D-Clear Native/SDS-PAGE electrophoresis. The gels were either stained by Coomassie Brilliant Blue (CBB), photographed, dried and exposed to phosphoimager plate, or blotted to a PVDF membrane and Ycf48 and D1 proteins were sequentially detected using specific antibodies (segments of the blot containing individual antibody signals are shown). Pigmented complexes were detected in the first dimension by their color (1D c) and fluorescence (1D f). Designations of complexes are as in Fig. 1. Arrows designate unassembled mature D1.

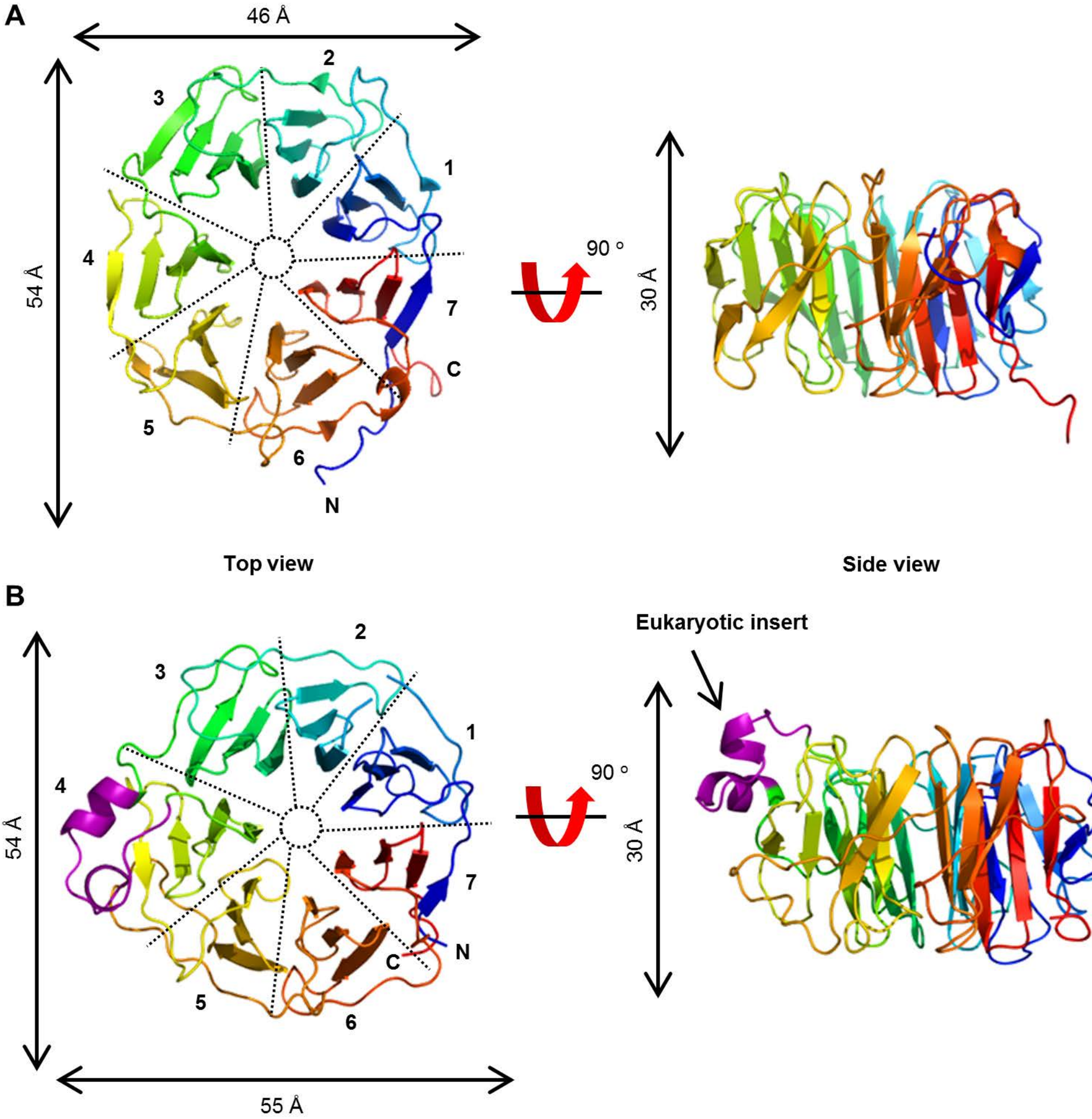
Fig. 6 Ycf48 and CyanoP protein are co-purified with FLAG-tagged YidC insertase. The FLAG-specific eluate obtained after purification of membrane proteins from a strain containing FLAG-tagged YidC (YidC-FLAG) or from WT as a negative control was analyzed by SDS-PAGE and the gel stained by Coomassie Brilliant Blue (left). Equivalent elutions were separated by SDS-PAGE and sequentially immunoblotted with a range of specific antibodies (right, segment of the blot with signals of each antibody is shown). The most intensively stained band was identified by protein mass-spectrometry as the bait (YidC-FLAG).

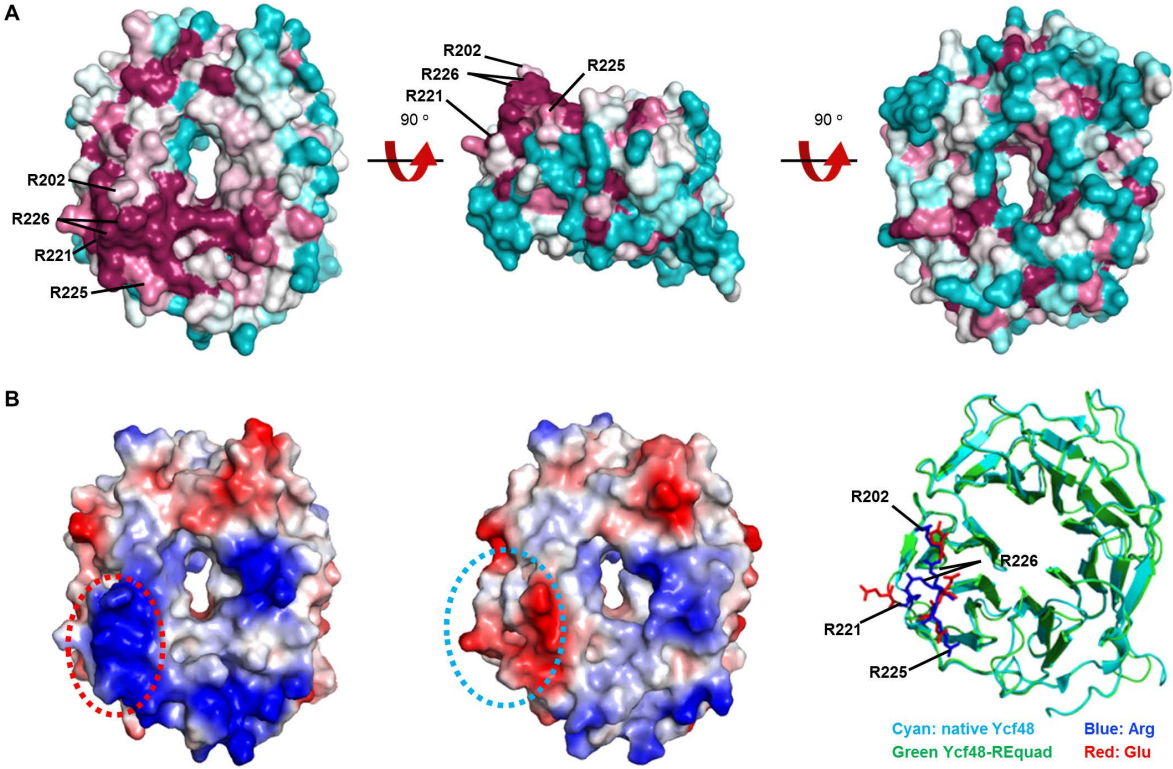
Fig. 7 Enhanced chlorophyll biosynthesis restores accumulation of chlorophyll-protein complexes in the Ycf48 mutant. (A) Levels of chlorophyll precursors are dramatically reduced in ΔYcf48. Chlorophyll precursors were extracted from 2 mL of cells with OD_{750nm}=0.4 and quantified by HPLC equipped with two fluorescence detectors set on different excitation and emission wavelengths (chromatograms on the left and right, detailed methods described in (43)). Coproporhyrinogen III (Copro) and protoporphyrin IX (Proto) are the last common precursors for both chlorophyll and heme synthesis. The first committed intermediate of chlorophyll pathway is Mg-protoporphyrin IX (MgP), which is consequently methylated (MgPME). The MgPME is converted into divinyl protochlorophyllide (DV-Pchlide) and then into divinyl and monovinyl chlorophyllide (DV/MV-Chlide); chlorophyll is finally made by attachment of phytol to the MV-Chlide. (B) Elevated levels of Pchlide and Chlide in ΔYcf48 grown for 24 hours in the presence of 0.2 mM N-methyl-mesoporphyrin IX (ferrochalatase inhibitor). (C) The growth of ΔYcf48 cells at low irradiance (40-50 µE m^{-2} s^{-1}) in the presence or absence of 0.3 mM N-methyl mesoporphyrin IX, a ferrochelatase inhibitor. (D) Absorbance spectra of mutant cells before and after 24 hours in the presence of 0.2 mM N-methyl mesoporphyrin IX. (E) Clear Native-PAGE of membrane complexes isolated from the identical cultures shown in (D) and loaded on an equal cell number basis (~2 mL of cells, OD_{750nm}=0.5).

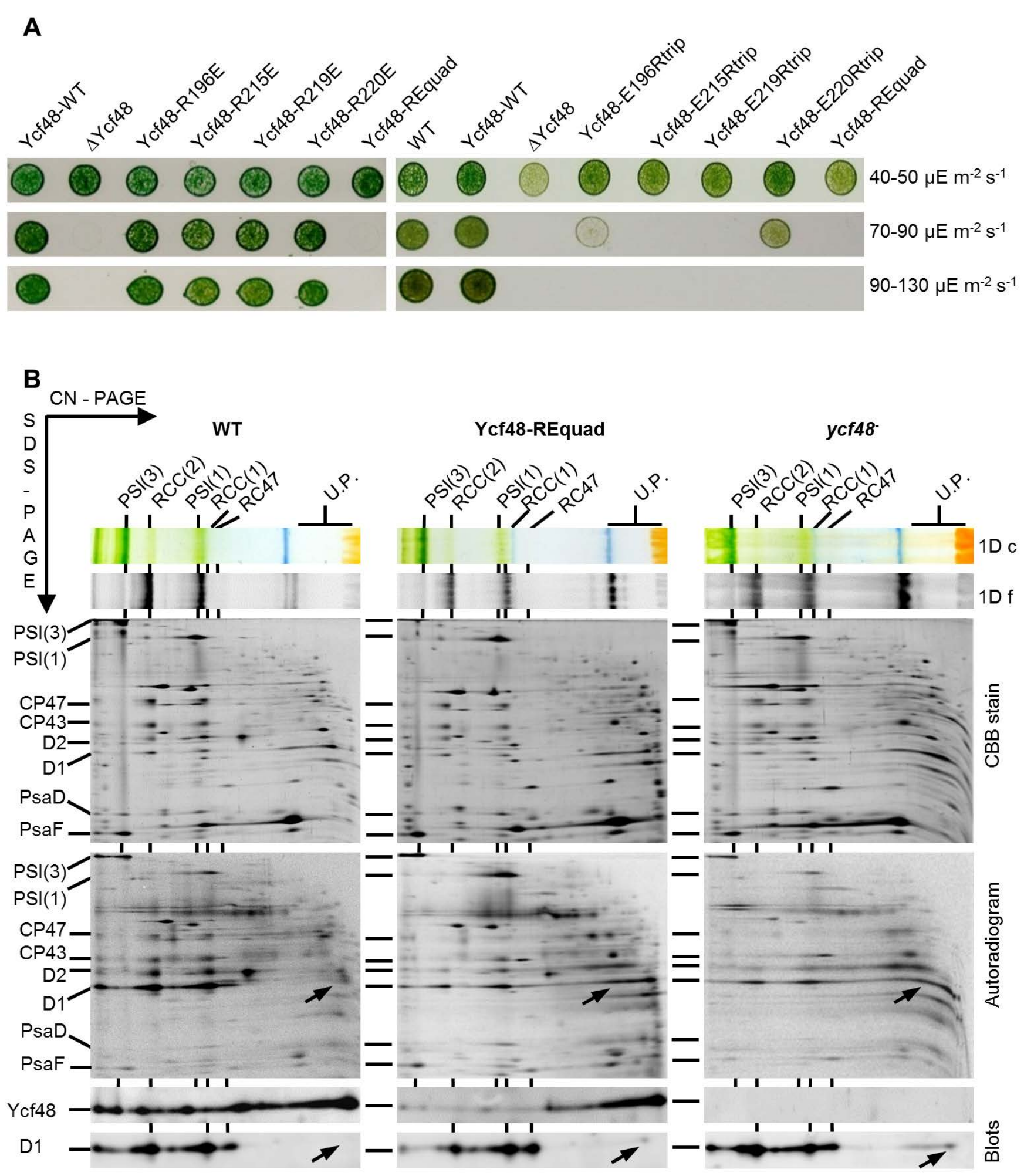
Fig. 8 Model for the role of Ycf48 in the synthesis of D1 and assembly of the PSII RCII complex. The potential mechanism of action of Ycf48 in PS II assembly is illustrated schematically. Ycf48 interacts with the C-terminal extension of precursor (pD1) and intermediate D1 (iD1), helping to synchronise D1 insertion via the YidC insertase, chlorophyll loading from chlorophyll synthase and C-terminal processing by the CtpA protease.

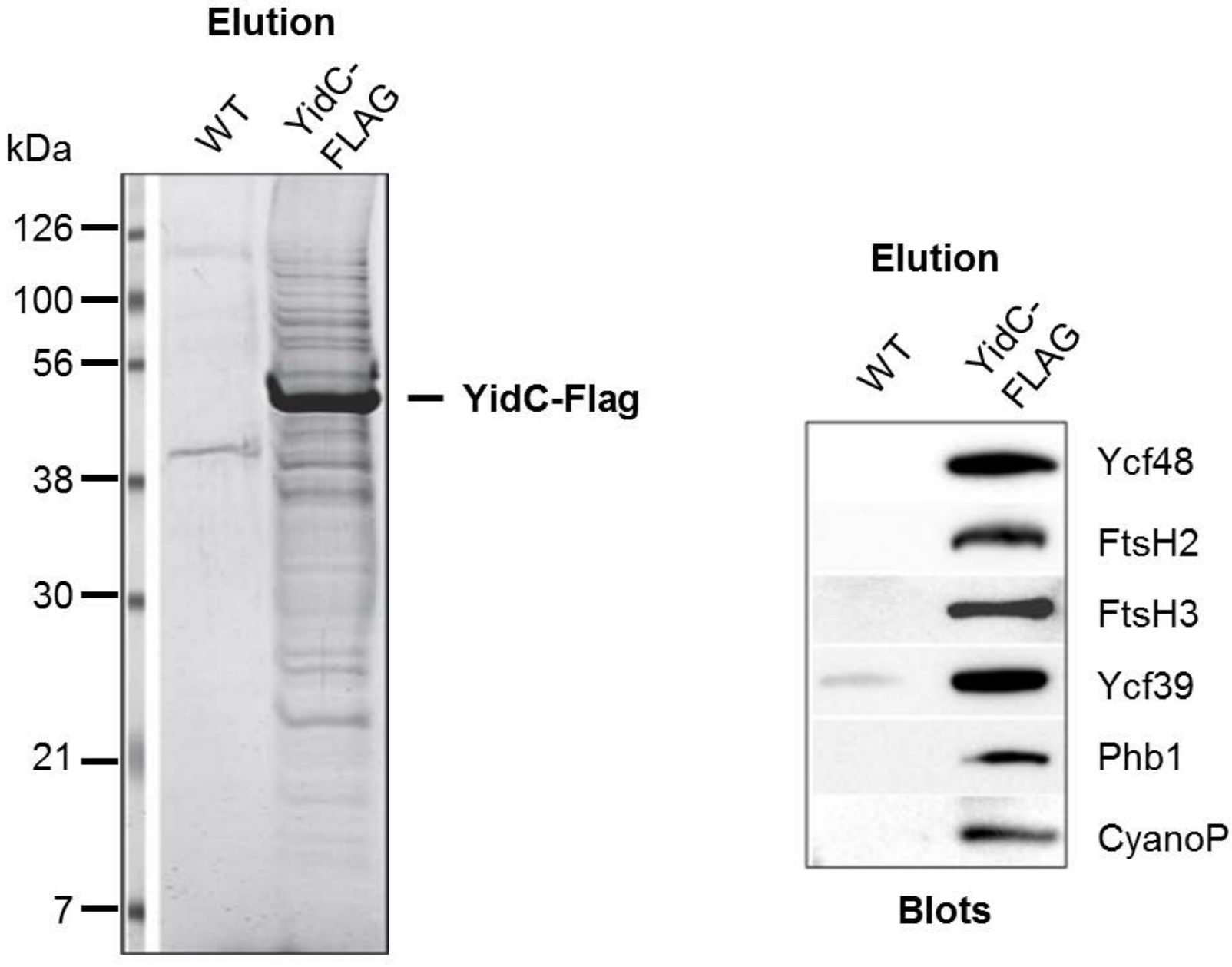

WT
CN - PAGE
SDS-PAGE
PSI(3)
RCC(2)
PSI(1)
RCC(1)
RC47
U.P.
1D color
1D fluor
CP47
Ycf48
CP43
D2
D1
PsaD
PsaF
PsaL
2D SYPRO stain
Ycf48
Blot
PSI(3)*
RCC(2)*
RCC(1)*
PSI(1)*
RC47*
RCII*
RCIIa

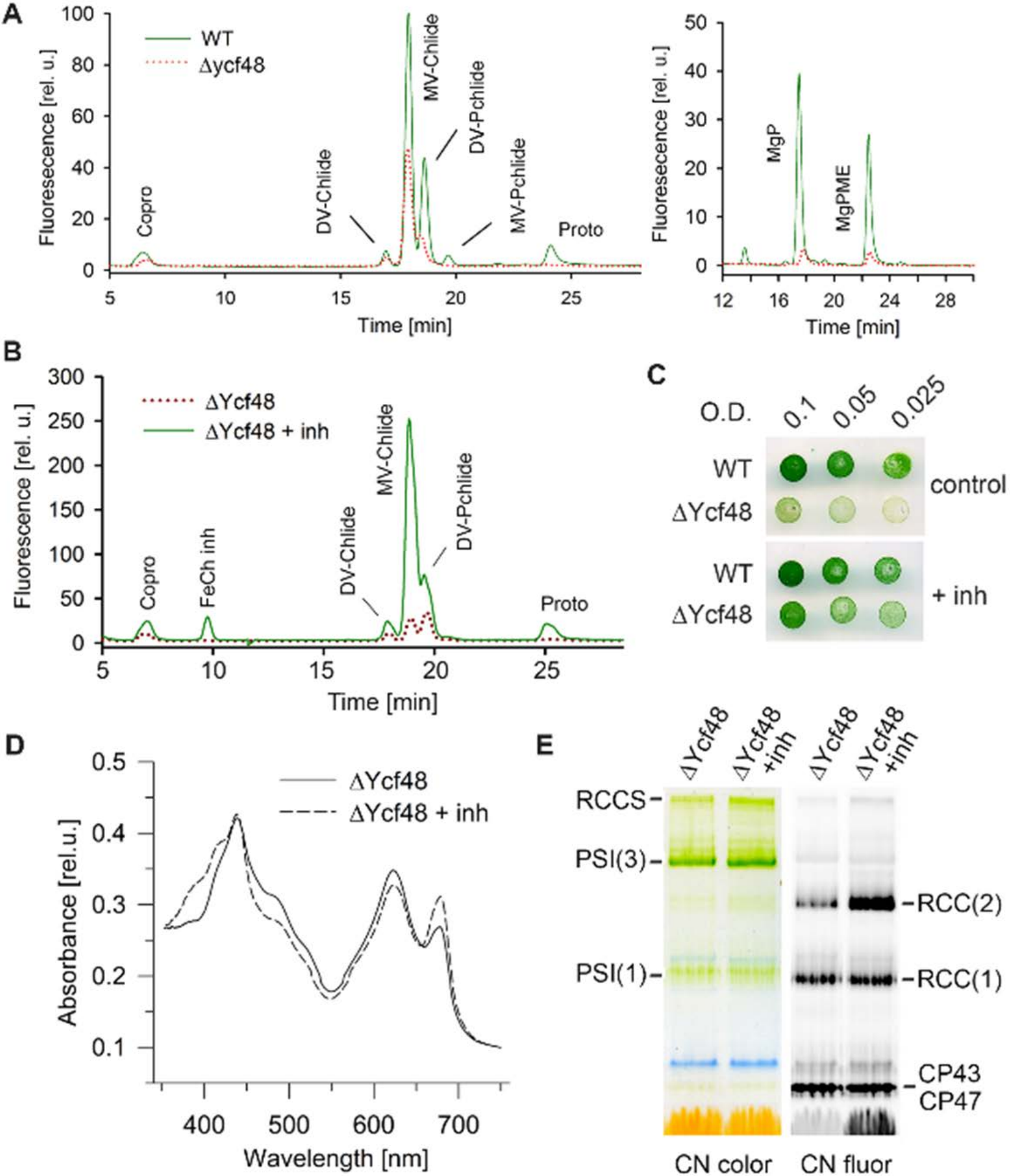

A
Membranes WT
Membranes ycf48-
GFP-Trap PSI-YFP
GFP-Trap WT
kDa
67
Ycf48
39
29
19
7
PsaA/B
PsaF-YFP denatured
PsaF-YFP
PsaD
PsaL
PsaE
αYcf48
αPsaD
αD1
B
CN - PAGE
SDS-PAGE
GFP-Trap PSI-YFP
PSI(3)
PSI(1)
U.P.
F.P.
1D color
αYcf48
αD1
GFP-Trap WT
PSI(3)
PSI(1)
U.P.
F.P.
1D color
αYcf48
αD1

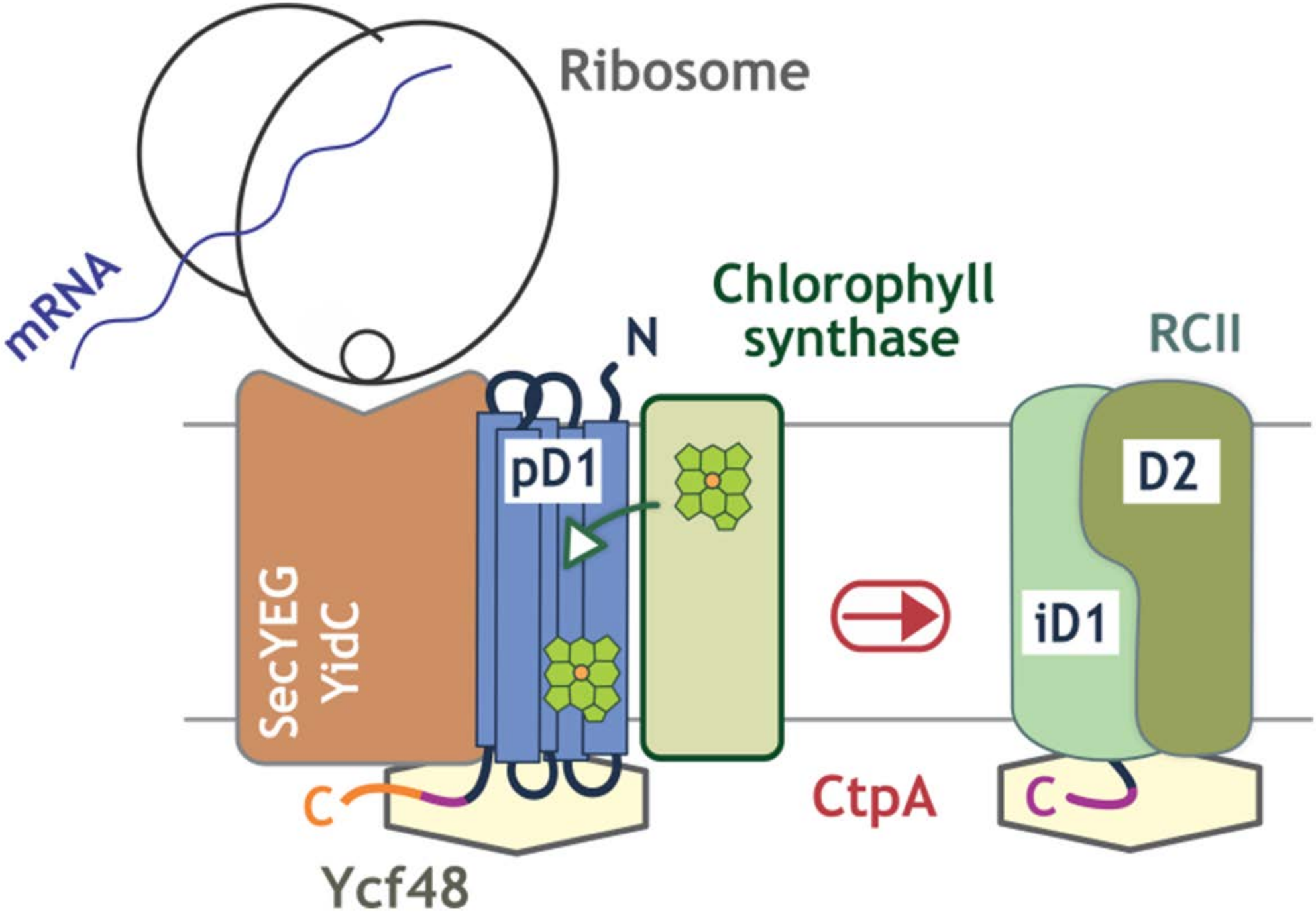

A
46 Å
54 Å
2
3
1
4
7
C
5
6
N
90 °
30 Å
Top view
Side view
B
Eukaryotic insert
2
3
1
4
7
N
C
5
6
54 Å
55 Å
90 °
30 Å


A
R202
R226
R221
R225
90 °
R202
R226
R221
R225
90 °
B
R202
R226
R221
R225
Cyan: native Ycf48
Green Ycf48-REquad
Blue: Arg
Red: Glu


A
Ycf48-WT
ΔYcf48
Ycf48-R196E
Ycf48-R215E
Ycf48-R219E
Ycf48-R220E
Ycf48-REquad
WT
Ycf48-WT
ΔYcf48
Ycf48-E196Rtrip
Ycf48-E215Rtrip
Ycf48-E219Rtrip
Ycf48-E220Rtrip
Ycf48-REquad
40-50 µE m-2 s-1
70-90 µE m-2 s-1
90-130 µE m-2 s-1
B
CN - PAGE
SDS-PAGE
WT
Ycf48-REquad
ycf48-
PSI(3)
RCC(2)
PSI(1)
RCC(1)
RC47
U.P.
1D c
1D f
PSI(3)
PSI(1)
CP47
CP43
D2
D1
PsaD
PsaF
CBB stain
Autoradiogram
Ycf48
D1
Blots


Elution
WT
YidC-FLAG
kDa
126
100
56
38
30
21
7
YidC-Flag
Elution
WT
YidC-FLAG
Ycf48
FtsH2
FtsH3
Ycf39
Phb1
CyanoP
Blots


A
WT
Δycf48
Fluoresecence [rel. u.]
Time [min]
Copro
DV-Chlide
MV-Chlide
DV-Pchlide
MV-Pchlide
Proto
MgP
MgPME
B
ΔYcf48
ΔYcf48 + inh
Fluorescence [rel. u.]
Time [min]
Copro
FeCh inh
DV-Chlide
MV-Chlide
DV-Pchlide
Proto
C
O.D.
0.1
0.05
0.025
WT
ΔYcf48
control
WT
ΔYcf48
+ inh
D
ΔYcf48
ΔYcf48 + inh
Absorbance [rel.u.]
Wavelength [nm]
E
ΔYcf48
ΔYcf48 +inh
ΔYcf48
ΔYcf48 +inh
RCCS
PSI(3)
PSI(1)
RCC(2)
RCC(1)
CP43
CP47
CN color
CN fluor


Ribosome
mRNA
N
Chlorophyll synthase
RCII
pD1
D2
SecYEG
YidC
iD1
C
CtpA
C
Ycf48